

Disorder-induced high-quality wavefront in an Anderson localizing optical fiber: supplementary material

BEHNAM ABAIE^{1,2}, MOSTAFA PEYSOKHAN^{1,2}, JIAN ZHAO³, JOSE E. ANTONIO-LOPEZ³, RODRIGO AMEZCUA-CORREA³, AXEL SCHÜLZGEN³, AND ARASH MAFI^{1,2,*}

¹Department of Physics & Astronomy, University of New Mexico, Albuquerque, NM 87131, USA

²Center for High Technology Materials (CHTM), University of New Mexico, Albuquerque, NM 87106, USA

³CREOL, College of Optics and Photonics, University of Central Florida, Orlando, FL 32816, USA

*Corresponding author: mafi@unm.edu

Published 8 August 2018

This document provides supplementary information to “Disorder-induced high-quality wavefront in an Anderson localizing optical fiber,” <https://doi.org/10.1364/optica.5.000984>. We further elaborate on the variance method used in the main text for M^2 calculations and discuss the numerical methods used for the simulation of the glass-Transverse Anderson Localizing Fiber (glass-TALOF). We also discuss the simulation results for an ideal TALOF. We show that for an ideal TALOF both the beam quality statistics and the distribution uniformity of the modes are improved. Finally, the experimental setup used for evaluating M^2 of the localized modes in glass-TALOF is described.

1. APPLICABILITY OF VARIANCE METHOD

In this section we elaborate on the variance method, which is used in the paper for calculation of M_x^2 and M_y^2 of the localized modes in the disordered fiber. As explained by Siegman in Ref. [1], it can be shown that the center of gravity of the beam (\bar{x}_1, \bar{x}_2) always travels rigorously in a straight line when diffracting in vacuum, if it is defined according to the first moment of the beam as

$$\begin{aligned}\bar{x} &= \iint dx dy (x I(x, y)), \\ \bar{y} &= \iint dx dy (y I(x, y)).\end{aligned}\quad (S1)$$

The universality and mathematically rigorous formulation of the variance method is the main reason behind its adoption for M^2 evaluation. It can be shown that the second moment of any finite beam obeys a universal, rigorous, quadratic free-space propagation rule of the form

$$\begin{aligned}\sigma_x^2(z) &= \sigma_{0x}^2 + \sigma_{\theta x}^2 \times (z - z_{0x})^2 \\ \sigma_y^2(z) &= \sigma_{0y}^2 + \sigma_{\theta y}^2 \times (z - z_{0y})^2,\end{aligned}\quad (S2)$$

where σ_{0x} and σ_{0y} represent the variance at the beam waist in the x and y directions; $\sigma_{\theta x}$ and $\sigma_{\theta y}$ are the variances of the angular spread of the beam departing from the waists; and z_{0x} and z_{0y} are the locations of the beam waist along the z axis. As stated in in Ref. [1], “this quadratic propagation dependence holds for any arbitrary real laser beam, whether it be Gaussian or non-Gaussian, fully coherent or partially incoherent, single mode or multiple transverse mode in character. Moreover, at least so far as anyone has proven, this quadratic dependence of beam width is rigorously true only for the second-moment width and not for any other of the width definitions listed above.” The second moment is calculated according to

$$\begin{aligned}\sigma_x^2 &= \iint dx dy (x - \bar{x})^2 I(x, y), \\ \sigma_y^2 &= \iint dx dy (y - \bar{y})^2 I(x, y),\end{aligned}\quad (S3)$$

where the beam is assumed to be normalized according to $\iint dx dy I(x, y) = 1$. The beam widths are defined as $W_x = 2\sigma_x$ and $W_y = 2\sigma_y$. The value of M_x^2 and M_y^2 are extracted from the

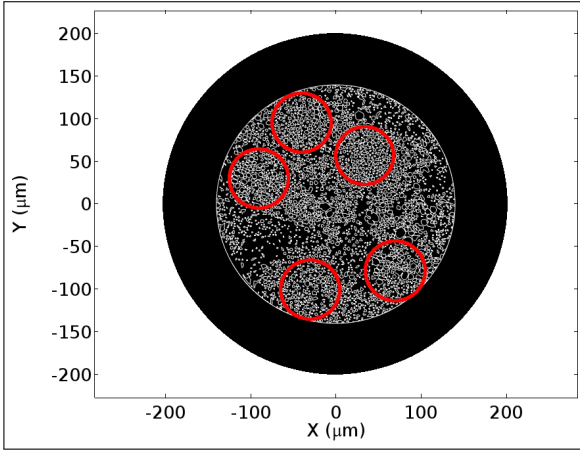


Fig. S1. Geometry of glass-TALOF. Red circles are the numerical domains used in Fig. 2e and Fig. 2f of the main text.

following expressions

$$W_x^2(z) = W_{0x}^2 + M_x^4 \times \left(\frac{\lambda}{\pi W_{0x}} \right)^2 (z - z_{0x})^2 \quad (\text{S4})$$

$$W_y^2(z) = W_{0y}^2 + M_y^4 \times \left(\frac{\lambda}{\pi W_{0y}} \right)^2 (z - z_{0y})^2.$$

2. NUMERICAL METHODS

A. Geometry of glass-TALOF

Figure S1 shows the geometry of glass-TALOF used in numerical simulations. In Fig. 2c and Fig. 2d of the main text, the entire geometry is imported to COMSOL and 1000 modes with the highest effective refractive index are calculated; the program was biased towards the modes located in the regions where lowest air fill-fraction exist and therefore the effective index of the material is larger in them. In order to overcome this problem, we choose to solve for the modes in regions with large air fill-fraction, separately. Red circles in Fig. S1 are representative of five individual domains that are used to calculate modes of the high air fill-fraction regions in Fig. 2e and Fig. 2f of the main text. Notice that, 100 modes of each domain is calculated individually where the circular domain is extracted and imported to COMSOL (COMSOL Multiphysics, COMSOL, Incorporated), separately. A scattering boundary condition is used to minimize the impact of outer boundaries of the individual domains on the results.

B. Impact of air fill-fraction

In this section we show the refractive index profile of an ideal TALOF described in the main text and compare the quality of modes in two TALOFs with different amounts of air fill-fraction (10% and 50% specifically). Fig. S2 shows the refractive index profile of an ideal TALOF [2, 3]. The fiber consists of a 100×100 array of unit cells with $a = 1 \mu\text{m}$ where a is the dimension of the unit cell. The refractive index of each unit cell is chosen randomly as either $n_1 = 1$ or $n_2 = 1.5$ with an equal probability. Fig. S2b is exactly the same fiber except for a case where the refractive indexes are not chosen with an equal probability. In this case, one out of ten pixels on average is randomly set to $n_1 = 1$ and therefore we end up with a structure, which has a 10% air fill-fraction.

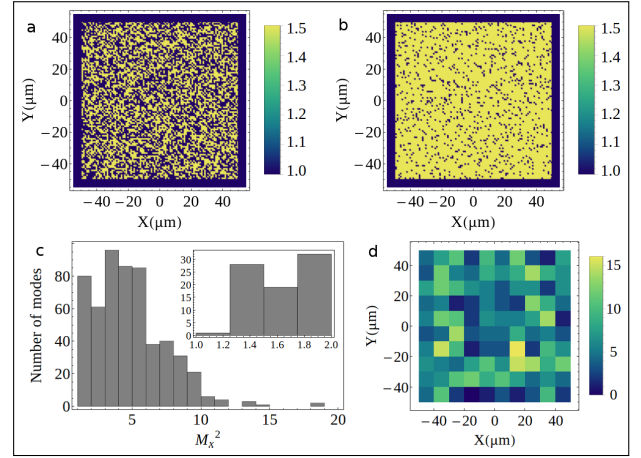


Fig. S2. a) Refractive index profile of an ideal TALOF with a uniform 50% air fill-fraction. b) Refractive index profile of a TALOF with 10% air fill-fraction. c) Histogram of the M_x^2 values for the 10% air fill-fraction. d) Density histogram of the location of the modes for the 10% air fill-fraction.

Figure S2c is representative of the histogram of 600 calculated modes in a fiber with Fig. S2b characteristics and its relevant density histogram, demonstrating the distribution of the modes is shown in Fig. S2d. The lower air fill-fraction has reduced the number of high quality modes. Please note that Fig. S2c should be compared with Fig. 3a of the main text. Based on previous analysis we expected this result; the ideal air fill-fraction for strongest localization is 50% based on the findings of Ref. [2]. It is quite expected that strongest localization automatically can result in improvement of the quality of the modes' wavefronts.

3. EXPERIMENTAL METHODS FOR EVALUATING M^2

The experimental setup used in the main text is demonstrated in Fig. S3. The output of a HeNe laser is coupled into a single-mode optical fiber (ThorlabsSM400). A high precision xyz translation stage (ThorlabsMAX343) is used to butt-couple the output of the single-mode fiber into a 155 cm long segment of glass-TALOF and scan the launch transverse position accurately across its input facet. The output of glass-TALOF is magnified by a 60x microscope objective. Light after the objective freely propagates and the beam profile is captured at different locations along the z axis by a CCD beam profiler.

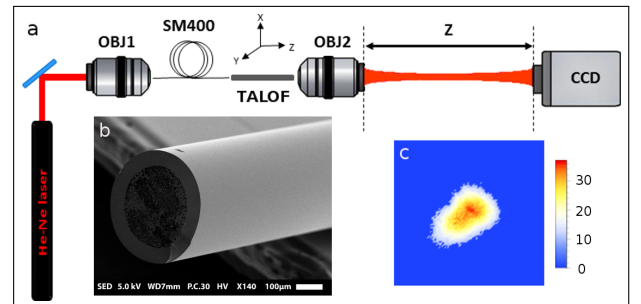


Fig. S3. Experimental setup for M^2 evaluation.

REFERENCES

1. A. E. Siegman How to (maybe) measure laser beam quality 1998 [online] Available:.
2. S. Karbasi et al., *Optics Express* **20**, 18692–18706 (2012).
3. S. Karbasi, R. J. Frazier, K. W. Koch, T. Hawkins, J. Ballato, and A. Mafi, *Nature Communications* **5** (2014).